ISBN: 978-3-95450-231-8 ISSN: 2673-5490 doi: 10.18429/JACoW-IPAC2023-THPM073

DUAL-SCATTERING FOIL INSTALLATION AT CLEAR

C. Robertson[1*], J. J. Bateman[1], M. Dosanjh[1], P. Korysko[1], University of Oxford, Oxford, UK
R. Corsini, W. Farabolini, A. Latina, A. Malyzhenkov,
V. F. Rieker[2], L. Wroe, CERN, Geneva, Switzerland
A. Gerbershagen, PARTREC, UMCG, University of Groningen, Netherlands
A. Aksoy[1], Ankara University, Ankara, Turkey
[1]also at CERN, Geneva, Switzerland
[2]also at University of Oslo, Oslo, Norway

Abstract

The CLEAR user facility at CERN allows users to receive a beam with energy up to 200 MeV, allowing flexibility in intensity, beam size and bunch structures. Separate from the main CERN accelerator complex, it is capable of hosting numerous experiments and catering to a broad array of needs with rapid installations at 2 test stands on the beamline.

The CLEAR beam is characteristically Gaussian when optimised for transport and a small transverse beam size. It would be highly desirable for many applications but particularly those of a medical nature, to be able to provide a 'flat' beam with a uniform intensity distribution over a significant component of its transverse component.

Over the CLEAR winter shutdown, the operators installed a dual-scattering system in the CLEAR beamline to provide this. It was placed several metres upstream of the beamline end to reduce X-ray contamination in the flattened beam and increase total transmission of the beam. Studies on the flattened beam composition in terms of structure and dose were carried out, also utilising a dipole directly upstream of the in-air test stand to separate the electron and X-ray beams for analysis.

INTRODUCTION AND BACKGROUND

CLEAR User Facility

CLEAR (CERN Linear Electron Accelerator for Research) is a 200 MeV electron beam user facility [1, 2]. Since its commissioning in 2018, it has been used in experiments for a number of applications including novel accelerator physics [3], beam diagnostics [4], and medical applications, particularly in the field of radiation therapy [5]. In the last decade, there has been much interest in combining very high energy electrons (VHEE) with the so-called FLASH modality, in which ionizing radiation is delivered at ultra high dose rates (UHDR) [6]. CLEAR experiments have been contributing to research in these fields [7].

Of particular note for medical experiments is the C-Robot on the in-air test stand at CLEAR. This remotely operated system is composed of three linear stages and a grabber. This can be used to hold samples or radiochromic films for irradiations and/or measurement of delivered dose. This allows many such irradiations to be carried out without intervening accesses to exchange films, saving time and allowing for greater efficiency [2].

The CLEAR beam has a characteristic Gaussian profile and can be modified using an extensive optics layout of quadrupoles through the beam line. Despite this flexibility, the maximum achievable beam size in CLEAR is small (a few mm). This is preferable during acceleration and propagation through the beam line, but it is desirable to have the ability to achieve a larger beam at the CLEAR in-air test area shown in Fig. 1. Additionally, experiments (particularly those based around radiation therapy) may benefit from a beam with a uniform transverse intensity profile, rather than a Gaussian profile. This can enhance conformality and greatly simplify the analysis of the dose provided by the beam.

Dual-Scattering Foil

One solution for providing a magnified and uniform beam is a dual-scattering foil. This concept has previously been utilised for particle therapy [8], and has regained interest as a method for providing large, flattened treatment beams. This interest is due to uncertainties around the interaction of the FLASH modality with the more commonly used spot-scanning method for tumour conformality in particle therapy, and difficulties in providing these in a UHDR timescale [9, 10].

In a dual-scattering system, a small initial beam passes through a flat foil or block of material. This increases the beam divergence, with the resultant angular phase space described by multiple scattering theory [11]. The angular distribution can be approximated as Gaussian, with the RMS contribution from the scatterer given by:

$$\theta_{\mathrm{RMS}} = 13.6\beta c p z \sqrt{\frac{x}{X_0}}\left(1 + 0.038 \ln\left(\frac{x z^2}{X_0 \beta^2}\right)\right) \qquad (1)$$

where z is particle charge (=1 for electrons), x is the longitudinal material thickness, X_0 is the material radiation length, p is the particle momentum in MeV/c and β is the relativistic parameter [12]. The RMS of the original angular distribution is added in quadrature to Eq. (1) to give the final divergence profile.

The enlarged beam then passes through a second scattering foil. Unlike the first, the second foil has a non-uniform shape, designed to preferentially scatter the centre of the beam outwards, thus transforming the Gaussian intensity

* cameron.robertson@physics.ox.ac.uk

ISBN: 978-3-95450-231-8 ISSN: 2673-5490 doi: 10.18429/JACoW-IPAC2023-THPM073

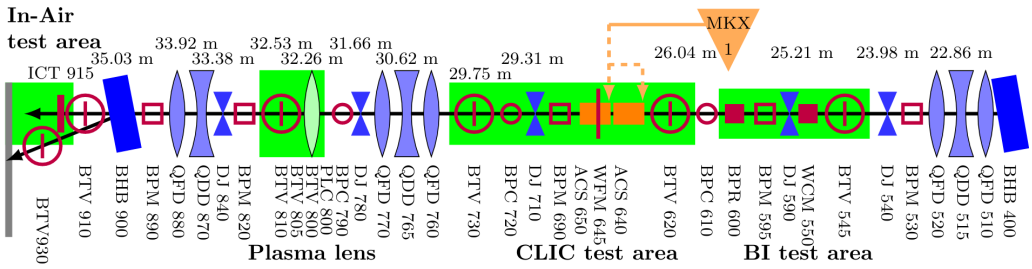

Figure 1: Experimental Beamline at CLEAR [1], beam moving right to left.

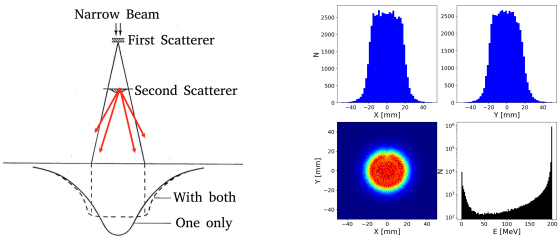

Figure 2: Dual-scattering foil concept [13] (left) and predicted transverse beam distribution at CLEAR in-air test stand from MC simulation in TOPAS (right).

profile to a constant intensity profile. In reality, this usually takes the form of a 3D Gaussian-like shape to complement the profile of the single-scattered beam [8]. A schematic of this dual-scattering process is shown in Fig. 2.

DESIGN AND INSTALLATION

The system was placed in vacuum in the CLEAR beam line rather than in the in-air test stand. This was to prevent additional obstructions in the test stand when the scattering system is used for experiments. Additionally, the positioning of the scattering system so close to any samples being irradiated would require thicker scatterers or higher-Z materials to magnify the beam significantly. This would result in increased losses and unwanted particle production. The current system was installed in two separate vacuum chambers upstream of the in-air test stand; the first scatterer placed directly upstream of QDD870, and the second scatterer inserted between QDD870 and QFD880 (elements visible in Fig. 1. Thus, only a small amount of scattering is be required to magnify the beam up to the size of the CLEAR beam pipe (20 mm radius). Furthermore, the CLEAR in-air dipole can be used to remove the electron beam component and measure the dose of any X-Ray contributions from Bremsstrahlung in the dual-scattering system.

Both scatterers were manufactured from Polyether ether ketone (PEEK). Its low density mitigates the requirements of manufacturing scatterers of very small dimensions whilst still exhibiting great radiation hardness [14]. The scattering system within the geometrical constraints in the beam line was designed using the TOPAS Monte Carlo code [15, 16], optimised using automated algorithms in Python.

For ease of manufacture and installation, the initial Gaussian shape of the second scatterer was divided into slices in this design process. The predicted beam distribution using generic initial conditions at CLEAR is shown in Fig. 2. These also include the simulation of thin mounting stems required for practical installation. The scatterers were manufactured and installed by members of the CLEAR operation team. The second scatterer was installed on an electronic linear stage with flexibility in the vertical position, while the first scatterer was installed on a simpler pneumatic stage with only two positions (in and out).

BEAM PROFILE MEASUREMENTS

Intensity Profile

Initial measurements of the transverse profile of the scattered beam were carried out using an yttrium aluminium garnet (YAG) screen held in place by the C-Robot in the beam line. Due to slight misalignments and lack of flexibility in the pusher for the transverse positioning of the first scatterer, and the jitter in the CLEAR beam, the dual-scattered beam was collimated heavily by the exit beam pipe before the in-air test stand. Furthermore, the positioning of the system resulted in the profile also being clipped by an extracted YAG screen in the beam pipe used during beam setup. Numerical images of the dual scattered beam are shown in Fig. 3 along with assorted profiles. Despite the clipping and screen blocking off some of the transmitted beam, an enlarged beam with a near-uniform component is clearly seen here. Some “overscattering” in Fig. 3 is clearly visible, resulting in a profile with a double peak rather than a flat top. This is a characteristic feature seen regularly during the design process simulations, and can be reduced by increasing the beam size on the first scatterer. However, due to the small size of the first scatterer and difficulty with alignment, it was difficult to carry this out systematically in these initial experiments.

These double peaks were far more severe in experiment than the TOPAS simulations. Modifications of the input beam parameters in TOPAS suggested that this was most likely due to differences in the beam emittance at CLEAR during the time of operation, compared to the approximate value used for the scattering system design.

Due to the beam size being much larger than could be fully measured on the YAG screens or dosimetric films, a steel

ISBN: 978-3-95450-231-8 ISSN: 2673-5490 doi: 10.18429/JACoW-IPAC2023-THPM073

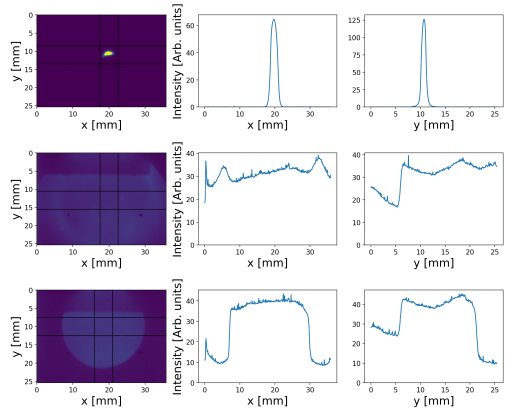

Figure 3: 2D and 1D (from shown slices) beam intensity profiles at CLEAR with open beam (top), dual-scattering system inserted (middle), and dual-scattering system and collimator inserted (bottom).

collimator with 22 mm full aperture was inserted into the setup to provide a beam profile of reduced size and smaller tails. The result of the collimation on the profile is also shown in Fig. 3, with the collimation also removing the portion of the beam profile clipped by the beam pipe.

The evolution of the beam uniformity in water was also investigated using the standard deviation across the beam intensity profile. The transverse collimated beam profile size was defined using a simple algorithm for identifying circular profiles via the OpenCV image processing library [17]. The standard deviation across slices of this identified circular profile were then calculated (neglecting the region affected by the screen impinging on the profile). The evolution of mean intensity and standard deviation is shown in Fig. 4, with the decreasing ratio of mean-standard deviation across a profile slice indicating the loss of flatness of the profile. The

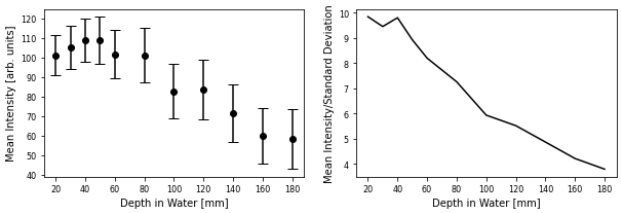

Figure 4: Evolution of mean profile intensity with increasing water depth, error bars represent standard deviation across profile (left), and mean intensity/standard deviation (right).

CLEAR in-air test stand dipole was used to investigate the production of any Bremsstrahlung solely from the scattering system. This is situated downstream of the scattering system installation, and was used to remove any charged component of the beam. However, any X-Ray profile on the YAG screen was far below the noise level seen on the C-Robot camera, even in water.

Dose Profile

Flattened dose profiles were also measured experimentally. This is be essential for the verifying dual-scattering foils as a method to provide enlarged and flattened treatment beams. GAFChromic EBT-3 radiochromic films were utilised for carrying out this measurement of flatness.

The 1D profiles of a sample dose measurement in air is shown in Fig. 5. Qualitatively, the dose profiles are uniform

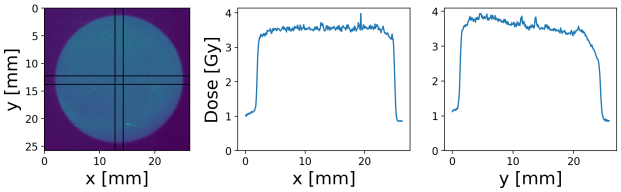

Figure 5: Dose profile from 10 nC accumulated charge through scattering system and collimator in air.

in x, while less so in y. Even with a slight misalignment resulting in asymmetry, the magnitude of the dose variance across the central region is still small compared with simulations of non-flattened beams. Quantitatively, the standard deviation across the dose profiles was calculated, although as these measurements were taken after realignment of the system to prevent the screen clipping, the standard deviation across the whole profile could be measured. Due to the careful alignment and removal of interfering screen in the dose measurement shown in Fig. 5, a mean dose μ=3.53 Gy with standard deviation σ=0.21 Gy across the whole beam profile defined by the OpenCV circle fit was calculated. This demonstrates the excellent uniformity achieved.

FUTURE WORK AND CONCLUSIONS

Such studies are crucial for medical applications, because the propagation of a flattened VHEE beam of a patient must be quantified and compared to simulations. This work has demonstrated that the dual-scattered beam at CLEAR was enlarged and mostly uniform, although depending moderately on alignment. This provided a dose profile with excellent uniformity in air.

A new scattering system is currently being manufactured to produce a smaller beam. This would result in a flat beam with a 10 mm flat radius, which should alleviate the clipping on the beam pipe, and allow more of the beam to be captured on the YAG and radiochromic films. The new scatterer will also allow depth-dose distributions in water to be captured, as enlargement of the beam in water from the current system would require larger YAG screens and films than those currently available at CLEAR. Simulations and experiments are also envisioned to explicitly quantify the variation of initial beam parameters on the resulting beam through a dual-scattering system situated significantly upstream of the patient. Further studies utilising the dipole can also be carried out to investigate the effects of dispersion on such a system, which would be of interest for the design of dual-scattering systems placed upstream of VHEE gantries.

ISBN: 978-3-95450-231-8 ISSN: 2673-5490 doi: 10.18429/JACoW-IPAC2023-THPM073

REFERENCES

[1] K. Sjobak *et al.*, "Status of the CLEAR electron beam user facility at CERN," MOPTS054, 2019. doi:10.18429/JACoW-IPAC2019-MOPTS054

[2] P. Korysko *et al.*, "Updates, Status and Experiments of CLEAR, the CERN Linear Electron Accelerator for Research," *JACoW IPAC*, vol. 2022, pp. 3022–3025, 2022. doi:10.18429/JACoW-IPAC2022-THPOMS030

[3] C. A. Lindstrøm *et al.*, "Emittance preservation in an aberration-free active plasma lens," *Phys. Rev. Lett.*, vol. 121, p. 194 801, 19 2018. doi:10.1103/PhysRevLett.121.194801

[4] A. Curcio *et al.*, "Noninvasive bunch length measurements exploiting cherenkov diffraction radiation," *Phys. Rev. Accel. Beams*, vol. 23, p. 022 802, 2 2020. doi:10.1103/PhysRevAccelBeams.23.022802

[5] K. Small *et al.*, "Evaluating very high energy electron rbe from nanodosimetric pbr322 plasmid dna damage," *Scientific Reports*, vol. 11, no. 1, pp. 1–12, 2021. doi:10.1038/s41598-021-82772-6

[6] P. Montay-Gruel *et al.*, "Irradiation in a flash: Unique sparing of memory in mice after whole brain irradiation with dose rates above 100gy/s," *Radiotherapy and Oncology*, vol. 124, no. 3, pp. 365–369, 2017, 15th International Wolfsberg Meeting 2017. doi:10.1016/j.radonc.2017.05.003

[7] R. Corsini, L. Dyks, W. Farabolini, A. Gilardi, K. Sjobak, and P. Korysko, "Status of vhee radiotherapy related studies at the clear user facility at cern," 2021. doi:10.18429/JACoW-IPAC2021-WEPAB044

[8] K. K. Kainz, J. A. Antolak, P. R. Almond, C. D. Bloch, and K. R. Hogstrom, "Dual scattering foil design for polyenergetic electron beams*," *Physics in Medicine & Biology*, vol. 50, no. 5, p. 755, 2005. doi:10.1088/0031-9155/50/5/002

[9] B. Rothwell, M. Lowe, E. Traneus, M. Krieger, and J. Schuemann, "Treatment planning considerations for the development of flash proton therapy," *Radiotherapy and Oncology*, vol. 175, pp. 222–230, 2022. doi:10.1016/j.radonc.2022.08.003

[10] S. Wei *et al.*, "Flash radiotherapy using single-energy proton pbs transmission beams for hypofractionation liver cancer: Dose and dose rate quantification," *Frontiers in Oncology*, vol. 11, 2022. doi:10.3389/fonc.2021.813063

[11] H. A. Bethe, "Molière's theory of multiple scattering," *Phys. Rev.*, vol. 89, pp. 1256–1266, 6 1953. doi:10.1103/PhysRev.89.1256

[12] G. R. Lynch and O. I. Dahl, "Approximations to multiple coulomb scattering," *Nuclear Instruments and Methods in Physics Research Section B: Beam Interactions with Materials and Atoms*, vol. 58, no. 1, pp. 6–10, 1991. doi:10.1016/0168-583X(91)95671-Y

[13] J. D. LeBlanc, "Design of electron dual foil scattering systems for Elekta Infinity radiotherapy accelerators," 2012. doi:10.31390/gradschool_theses.2440

[14] E.-S. A. Hegazy, T. Sasuga, M. Nishii, and T. Seguchi, "Irradiation effects on aromatic polymers: 2. gas evolution during electron-beam irradiation," *Polymer*, vol. 33, no. 14, pp. 2904–2910, 1992. doi:10.1016/0032-3861(92)90075-8

[15] J. Perl, J. Shin, J. Schumann, B. Faddegon, and H. Paganetti, "TOPAS: An innovative proton Monte Carlo platform for research and clinical applications," *Medical Physics*, vol. 39, p. 6818, 2012. doi:10.1118/1.4758060

[16] B. Faddegon *et al.*, "The TOPAS Tool for Particle Simulation, a Monte Carlo Simulation Tool for Physics, Biology and Clinical Research," *Physica Medica*, 2020. doi:10.1016/j.ejmp.2020.03.019

[17] G. Bradski, "The OpenCV Library," *Dr. Dobb's Journal of Software Tools*, 2000.